JOURNAL OF PROPULSION AND POWER
Vol. 23, No. 4, July–August 2007

Experimental Study of the Unstable–Unstarted Condition of a Hypersonic Inlet at Mach 6

Hui-jun Tan* and Rong-wei Guo†
Nanjing University of Aeronautics and Astronautics, 210016 Nanjing, People's Republic of China

DOI: 10.2514/1.28039

Wind-tunnel tests were conducted to better understand the flow pattern of a hypersonic inlet at an unstable–unstarted condition that is caused by the downstream mass flow choking. High-speed shadowgraph flow visualization and instantaneous pressure measurements are employed to reveal the oscillations of the shock system and the unsteady process of the duct flow. Results show that the shock system both inside and in front of the inlet duct oscillates intermittently when the inlet is unstarted. With the increase of the downstream throttling ratio, the fundamental frequency of the unsteady flow process goes up and the shock-on-lip time goes down, but the process whereby the shock system is disgorged and swallowed remains unchanged, lasting for 15 ms. When the throttling ratio is 89 and 91%, the fundamental frequency is 8 and 23 Hz, respectively. At the smaller throttling ratio, the aerodynamic oscillatory phenomenon of the inlet can be divided into three stages: namely, mass filling up, shock system disgorging and swallowing, and near-throat flow pattern establishing and backpressure propagating. At the larger throttling ratio, the first stage disappears and the third one shortens.

Introduction

HYPERSONIC inlets should always operate in a started mode for proper operation. But owing to the immaturity of the design methods, the inaccuracy of the CFD tools, the inconsistency between the ground-simulated and flight conditions, and the uncertainty of the engine thrust regulations, the unstarted conditions of inlets inevitably occur during the development of hypersonic airbreathing propulsion systems. When unstarted, hypersonic inlets suffer from an abrupt reduction in captured airflow and total pressure efficiency and an abrupt increase in aerodynamic loads and thermal loads [1]. Over the past few decades, the starting problems of hypersonic inlets have been studied extensively [2–9]. Great efforts have been made to establish a method for the accurate prediction of starting, self-starting, and maximum-contraction ratios of hypersonic inlets. Some approaches have also been attempted for the improvement of the starting and restarting capability of hypersonic inlets. Unfortunately, several papers have focused on the flow pattern of unstarted hypersonic inlets [10–12] and dealt with this phenomena mainly in a steady manner, which blurs its oscillatory nature and diminishes its possible threat artificially. In [13], the mean and time-accurate pressures in a two-dimensional hypersonic inlet were measured both under a backpressure-induced unstart condition and under a cowl-induced unstart condition. Some useful conclusions were obtained, but due to the insufficiency of dynamic pressure gauges and the lack of flow visualization, the unsteady flow pattern of a hypersonic inlet is still obscure. What's worse, even the authors of [13] are not sure whether the observed unsteady pressure behavior is the result of noisy measurements. As to the flow pattern of unstarted supersonic inlets, many papers have discussed the buzz phenomena and analyzed the possible oscillatory mechanisms, which are not agreed upon even at present [14–16]. In general, the progress achieved in unsteady flow of supersonic inlets is remarkable and valuable. But for an unstarted hypersonic inlet, the flow pattern can be quite different from that of an unstarted supersonic inlet. The expelled shock system of the latter contains a normal shock, but the former does not. As a result, flow is spilled subsonically for supersonic inlets but supersonically for hypersonic inlets (Fig. 1) [1]. What's more, unstarted hypersonic inlets are more likely to exhibit remarkable shock system oscillations and corresponding prominent pressure fluctuations both inside and in front of the internal ducts, which are highly detrimental to the stable operations of ramjets or scramjets.

In this paper, an experimental study is conducted on the aerodynamic instability of an unstarted hypersonic inlet, which is caused by the mass flow choking near the plug downstream, at a Mach number of 6. High-speed shadowgraphs and instantaneous static pressures along the duct are employed to reveal the oscillations of the shock system and the unsteady process of the duct flow.

Experimental Setup

Wind Tunnel

The experiment is conducted in a pulse-type combustion-heated wind tunnel. The facility runs in a blown-down mode and the usable runtime is greater than 200 ms. The test chamber is fully closed with schlieren glass windows for optical access, for which the diameter is 300 mm and the center is 260 mm downstream of the nozzle exit. An axisymmetric converging–diverging supersonic nozzle with a diameter of 600 mm at the exit is located upstream of the test chamber, providing a nominal freestream Mach number of 6. According to wind-tunnel calibrations, the diameter of the uniform flow region at the exit of the nozzle is Φ440 mm and greater than Φ320 mm at the station 500 mm downstream. The total temperature of the freestream is 1650 K, total pressure is 3.0 MPa, and unit Reynold number is $3.65 \times 10^6/\text{m}$. At the exit of the nozzle, the specific heat ratio is 1.35 and the gas constant is 315.83 $\text{J}/(\text{kg} \cdot \text{K})$.

Inlet Model

The inlet model used in the experiment simulates the inlet system for ramjet modules of a dual-combustor ramjet. The inlet is designed for a shock-on-lip Mach number of 6.0 and for a self-starting Mach number of 3.0. The outside compressions are accomplished by a cone surface with two turnings, for which the initial half angle is 14 deg and the two following turning angles are both 5 deg. The total area contraction ratio of the inlet is 7.0 and the internal ratio is 1.5. Downstream of the throat of the inlet, a 3-D variable section duct for which the area ratio (exit section to inlet section) is 1.4 serves as the subsonic diffuser.

Received 26 September 2006; revision received 21 April 2007; accepted for publication 21 April 2007.

*Associate Professor, College of Energy and Power Engineering.
†Professor, College of Energy and Power Engineering.

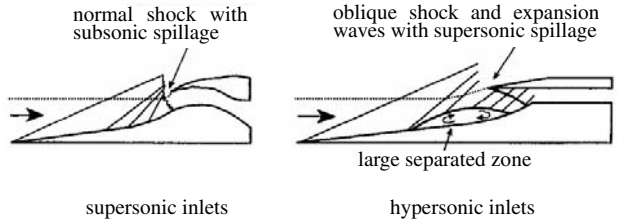

Fig. 1 Flow patterns of mixed-compression inlets at unstarted conditions [1].

Figure 2 illustrates the test model in which the full flowpath of two inlets for the ramjet is embodied with a cowl-lip diameter of 300 mm. The entrance areas of the four inlets for the scramjet are also installed to take into account the possible interactions. Two streams captured by the inlets for the ramjet impinge at the dump combustor and are discharged through a long straight duct with a slenderness ratio of 10:1. At the end of the straight duct, a conical plug is placed to alter the backpressure of the inlet. Flow captured by four inlets for the scramjet outflows from the model directly after passing the entrance area.

Experimental Measurements

Instantaneous static pressure measurements are performed by 48 dynamic pressure (Kulite®) gauges (27 stations on the central body-side surface and 21 stations on the cowl-side surface) to monitor the unsteady flow pattern inside inlet A. Pitot pressure rakes are mounted at the end of the throat of inlet B and at the exit of the inlet A to obtain the time-accurate local total pressure and local Mach number. Also, several dynamic pressure gauges are used to monitor the operation process of the wind tunnel, such as the action of hydrogen value, the action of oxygen value, and the establishment of the total pressure of the prechamber.

The data sampling frequency is 11 KHz. To obtain the concerned instantaneous pressure information and also to ensure the entire operation process of the wind tunnel being monitored, the sampling process lasts for 3 s. As far as the pressure gauges are concerned, the cutoff frequency is as high as 50 KHz. But during tests, the cavum in the sensor and the conduit degrade the frequency response of the data acquisition system. The volume of the cavum in the sensor is 40 mm^3 and the longest conduit used does not exceed 100 mm, and so according to a conservative estimate, the cutoff frequency of the system is higher than 1159 Hz, taking the speed of sound as 300 m/s. In general, the cutoff frequency of the data acquisition system should be three times the interested frequency of the signal or higher, and so in this paper, the analysis of a dynamic signal less than 386 Hz is authentic.

The behavior of the shock system in front of the internal duct is recorded by high-speed shadowgraph flow visualization, with a sampling rate of 400 frames per second. Because of the memory limit, the charge-coupled device (CCD) camera used can only work 120 ms per test, and so synchronization between the camera and the wind tunnel is performed. Figure 3 shows a typical time sequence of the experiment according to the time history of the prechamber total pressure, for which zero on the time axis represents the start of the data sampling process.

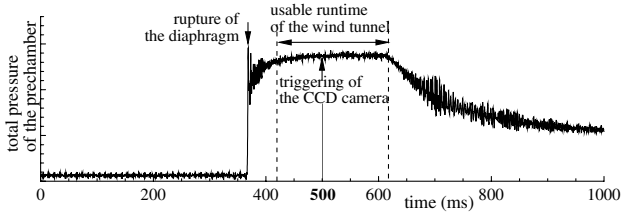

Fig. 3 Typical time sequence of the experiment.

Results and Discussion

The inlet operating conditions are varied by changing the position of the backplug, which controls the exit area of the flowpath. The backplug position is identified by the throttling ratio (TR), defined as the ratio of the throat area near the plug to the cross-sectional area of the straight duct. During tests, the throttling ratio can be varied between 0% (fully opened) and 100% (fully closed). What's more, each experiment is repeated twice for credible results.

Throttling Ratios from 0 to 87%

Before plunging into the unstable–unstarted condition of the hypersonic inlet, it is worthwhile to first discuss the started inlet flowfield. Over the past few decades, many papers have concerned this specific problem. Oh et al. [17] gave a very detailed presentation on a supersonic inlet flowfield, focusing on the response of inlet aerodynamics to externally imposed pressure oscillation at the diffuser exit.

For the hypersonic inlet studied in this paper, a stable–started condition can be obtained when the TR ranges from 0 to 87%. As shown in Fig. 4, the time-averaged static pressure distributions along the internal surfaces continue to climb up and the initial disturbed points keep on moving toward the cowl lip with the increase of the TR, indicating the traveling upstream of the internal shock train. The time-averaged static pressure at the exit plane of the diffuser peaks at a TR of 87%. Analysis of the time history shows that the pressure

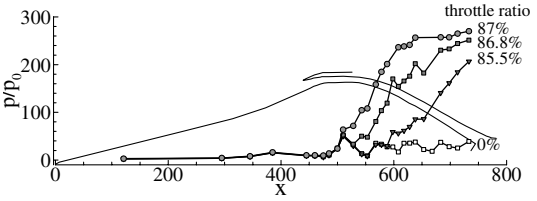

a) Central body-side surface

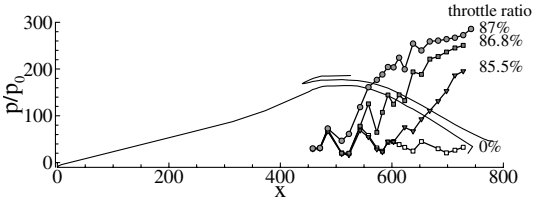

b) Cowl-side surface

Fig. 4 Distributions of time-averaged surface static pressure when the TR ranges from 0 to 87%.

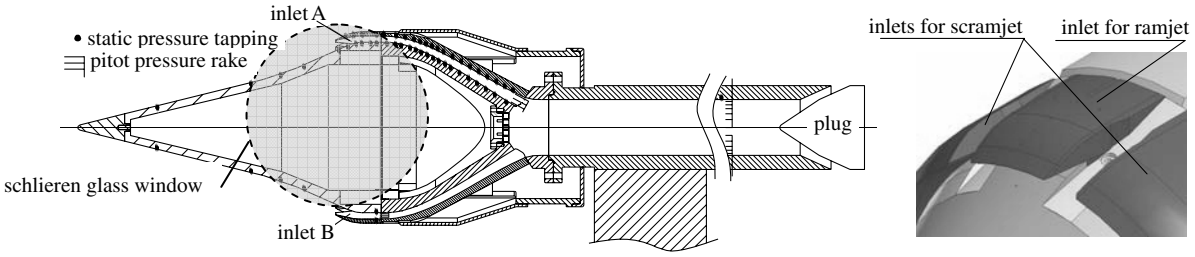

Fig. 2 Test model.

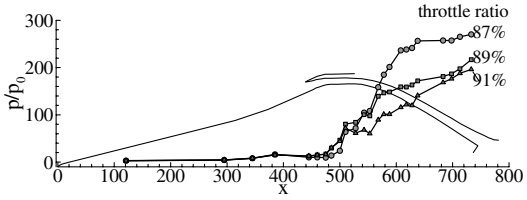

a) Central body-side surface

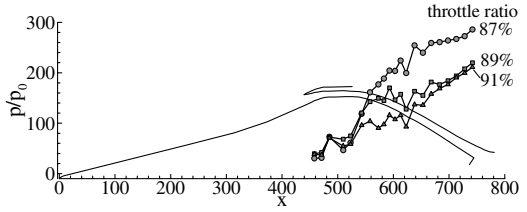

b) Cowl-side surface

Fig. 5 Distributions of time-averaged surface static pressure when the TR overruns 87%.

fluctuation of each measure point is fairly small and the maximum p_{rms} is less than 1.0% of the freestream total pressure. Shadowgraphs show that the external shocks remain on the lip the entire time.

Throttling Ratio of 89%

When the throttling ratio changes from 87 to 89%, time-averaged static pressure near the exit of the inlet descends remarkably and the initial disturbed points of wall static pressure go upstream to the entrance of the internal duct, suggesting that the inlet is unstarted (Fig. 5).

Shadowgraphs show that the shock system in front of the inlet is disgorged and swallowed intermittently when the throttling ratio increases to 89%. As shown in Fig. 6, the scope of the shock oscillations is large and the external compression shocks are once deformed into one strong curved shock. It can also be noticed that no normal shock is observed during the oscillations, which is different from supersonic inlets. In the valid visualization period, which lasts for 120 ms, the reciprocation of the shock system is observed only once (Fig. 6), indicating that the shock system oscillates at a frequency lower than 8.5 Hz. In fact, the rapid motion of the external shock system lasts for only 15 ms, and most of the time, the shock system remains on the lip.

The static-pressure–time history of the last survey point on the central body surface is exhibited in Fig. 7. It can be noted that after a platform of about 60 ms, the instantaneous static pressure descends and ascends rapidly and remarkably and then takes on a near-steady process again. At a condition of 3.0 MPa freestream total pressure, the static pressure fluctuating range is as high as 176 KPa and increases proportionally with the freestream total pressure. This periodical aerodynamic load is a big threat to the structure safety of the inlet and even to that of the aircraft. Power spectrum analysis of the pressure–time history (Fig. 8) shows that most of the fluctuating energy is contained below 100 Hz and a prominent peak of power spectral density appears near 8 Hz, which is consistent with the result

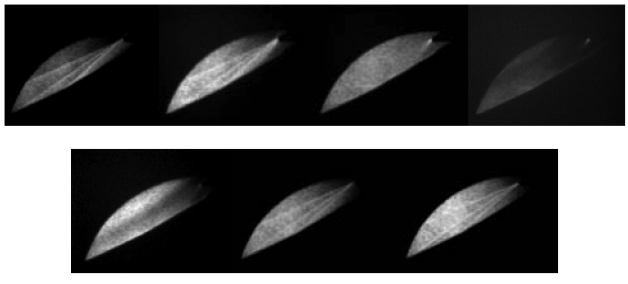

Fig. 6 Process of shock system being disgorged and swallowed; the TR is 89% and the time interval is 2.5 ms.

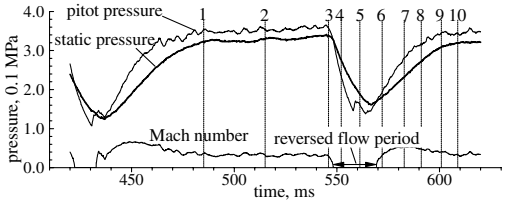

Fig. 7 Static-pressure–time history of the last survey point on the central body-side surface; the TR is 89%.

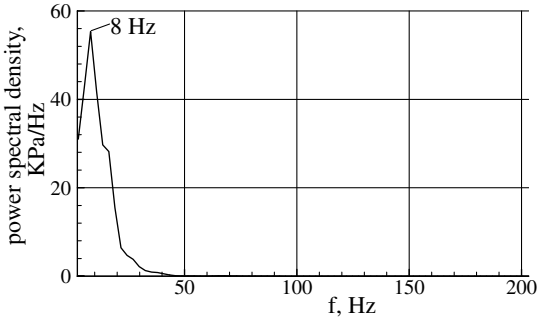

Fig. 8 Spectral density distribution of instantaneous surface static pressure; the TR is 89%.

of shadowgraphs observations. Based on the concept of a Helmholtz resonator, the frequency of the unsteady flow in the inlet is estimated by the equation

$$f = \frac{a}{2\pi}\sqrt{\frac{A}{LV}}$$

where a and A are typical values of the sound speed and cross-sectional area in the inlet, L is the length of the internal flowpath, and V is the fluid volume inside the inlet model. Calculations show that the Helmholtz resonator frequency for this inlet model is 50 Hz, which is considerably higher than the observed frequency of 8 Hz. So the oscillation observed here is not a Helmholtz resonator system, but a complex phenomenon that is closely related to the internal and external flowfield of the inlet.

Actually, the flow pattern of the inlet changes moment by moment. Instantaneous static pressure distributions along the central body-side surface at different typical moments (Fig. 7) are shown in Fig. 9. The integral time is chosen as 2 ms when calculating the instantaneous static pressure to achieve sufficient time resolution. In Fig. 9, the distribution of time-averaged wall static pressure at a throttling ratio of 87%, when the inlet operates at a steady near-critical condition, is shown with a thick solid line for reference. According to Fig. 9, the oscillation cycle of the unsteady flowfield can be divided into three stages: namely, mass filling up (485th–546th milliseconds), shock system disgorging and swallowing (546th–561st milliseconds), and near-throat flow pattern establishing and backpressure propagating (561st–609th milliseconds).

Mass Filling Up (485th–546th Milliseconds)

When the throttling ratio is 89%, the mass filling-up stage is the longest stage and lasts for 61 ms. At this stage, the external shock system is fully on the cowl lip and the captured mass flow is slightly larger than the discharged mass flow at the duct exit, leading to a slow accumulation of airflow in the duct and an ever-increasing backpressure at the exit section of the inlet. Lines marked with 1–3 in Fig. 9 denote the instantaneous static pressure distributions at the start, the middle, and the end moments of the mass filling-up stage. It can be noted that line 1 overlaps with the time-averaged pressure distribution of 87% throttling ratio when the leading edge of shock train is at the end of the throat. So at this moment, the external and the internal shock systems of the inlet are established and the flow pattern is the same as that of steady near-critical operating condition. Then

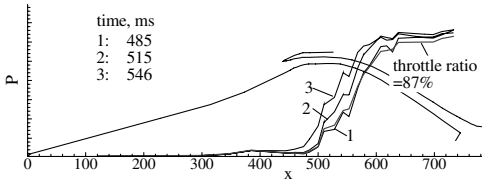

a) Mass filling-up

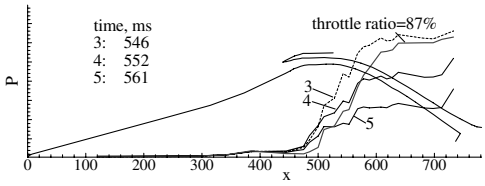

b) Shock system disgorging and swallowing

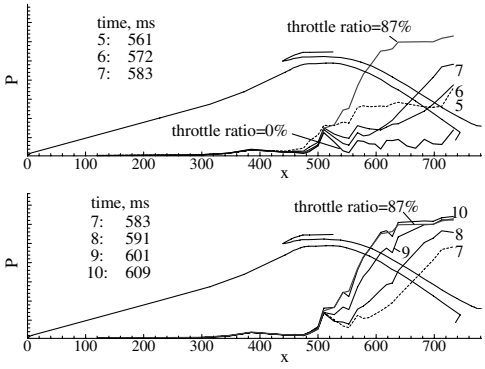

c) Near-throat flow pattern establishing and back pressure propagating

Fig. 9 Distributions of instantaneous static pressure along the central body-side surface at different typical moments; the TR is 89%.

the augment of the backpressure forces the internal shock system of the inlet to move upstream slowly. Line 2 shows that after 30 ms, the leading edge of the shock train is pushed to the middle section of the throat. After 31 more milliseconds, the leading edge of the shock train reaches the forepart of the contract area of the inlet (line 3) and the next stage begins.

Figure 7 also gives the time histories of the pitot pressure (measured by the pitot tube 2 mm away from the wall) and the deduced local Mach number at the exit of inlet A. Note that at the mass filling-up stage, the Mach number at the exit of the inlet is fairly stable and fluctuates slightly round 0.33.

Shock System Disgorging and Swallowing (546th–561st Milliseconds)

This stage is the most impressive, though it lasts for only 15 ms. At this stage, shock systems of the inlet are disgorged and swallowed rapidly (Fig. 6) and parameters of the internal flow change sharply.

When the shock train is expelled out of the internal duct, the motion of the shock system is speeded up remarkably. Only 6 ms after the mass filling-up stage, the shock system is disgorged entirely and the captured mass flow of the inlet descends distinctly. Then due to the imbalance of less captured mass flow and nearly unchanged discharged mass flow, a pressure trough is formed near the plug and propagates upstream, leading to a remarkable static pressure drop at the aft area of the inlet (line 4). Six more milliseconds later, with the aid of the formed static pressure drop, the disgorged shock system is swallowed into the internal duct and the external shocks remain on the lip again, which is indicated by the fall of wall static pressure at the entrance and at the throat of the inlet (line 5).

It can be noted from Fig. 7 that at the moment of the shock system being disgorged, the Mach number at the exit of the inlet decreases sharply and then the reversed flow period appears, which lasts for 20 ms and persists until the third stage. Reversed flow at the exit of the inlet is very dangerous, because hot gas of the combustor may be brought back to the inlet, for which no thermal protection is adopted.

Near-Throat Flow Pattern Establishing and Backpressure Propagating (561st–609th Milliseconds)

The pressure trough formed at the second stage continues to propagate upstream and results in a further pressure drop near the throat of the inlet. The diminishing gaps between pressure-distribution lines at this stage and that at 0% throttling ratio near the throat indicate that at this stage, the started flow pattern near the throat of the inlet is reestablished gradually. The low-speed region near the throat formed at the second stage is reaccelerated to a supersonic speed and the internal shock train downstream of the throat appears again. At the same time, the captured mass flow is blocked near the backplug and an instantaneous high pressure is formed. This pressure peak propagates upstream and results in an ever-increasing backpressure at the exit of the inlet, which forces the shock train in the diffuser to move upstream continually. When the leading edge of the shock train situates at the end of the throat, a new cycle begins.

Reviewing the preceding analysis, the shock system can be swallowed easily after being disgorged and the started flow pattern can be reestablished rapidly, and so it can be inferred that the inlet studied here has the ability of self-starting at a Mach number of 6.

Throttling Ratio of 91%

When the throttling ratio increases to 91%, the time-averaged static pressure of the duct goes down further (Fig. 5). Shadowgraphs show clearly that the shock system at the entrance of the inlet still oscillates. But the cycle is shortened greatly and lasts for only 40 ms, of which the process of shock system disgorging and swallowing occupies 15 ms (Fig. 10) and the shock-on-lip process takes up 25 ms. Compared with the condition of 89% throttling ratio, the shock-on-lip process becomes obviously shorter, but the other remains nearly unchanged at a throttling ratio of 91%.

The static-pressure–time history of the last survey point on the central body-side surface at a throttling ratio of 91% is shown in Fig. 11. The periodic behavior of the instantaneous pressure is more remarkable. But the platform that indicates the mass filling-up stage disappears and the pressure fluctuating range declines to a typical value of 157 KPa at a condition of 3.0 MPa freestream total pressure. It can also be noted that reversed flow still exists at the exit of the inlet, occupying nearly 40% time of the entire cycle. The power spectrum density of the pressure–time history is demonstrated in Fig. 12. It can be seen from this figure that most of the fluctuating energy is distributed below 100 Hz and the fundamental frequency is 23 Hz.

Figure 13 illustrates typical distributions of instantaneous static pressure at a throttling ratio of 91% (refer to Fig. 11). Mass imbalance becomes more evident due to the shrink of the throat area near the backplug, and as a result, the mass filling-up stage becomes unapparent. Near-throat flow pattern establishing and backpressure propagating is also affected by the variation of the throttling ratio. The duration is shortened from 48 to 29 ms, whereas the throttling ratio increases from 89 to 91%. But shock system disgorging and swallowing seems unresponsive to the variation of the throttling ratio

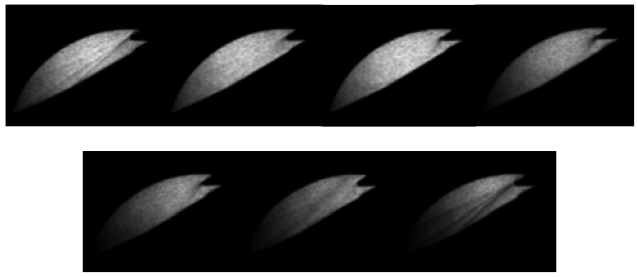

Fig. 10 Process of shock system being disgorged and swallowed; the TR is 91% and the time interval is 2.5 ms.

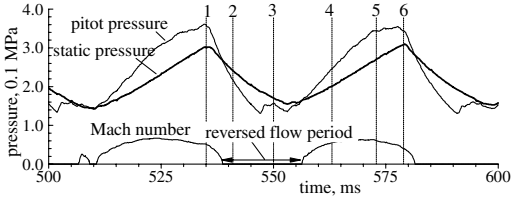

Fig. 11 Wall static-pressure–time history of the last survey point on the central body-side surface; the TR is 91%.

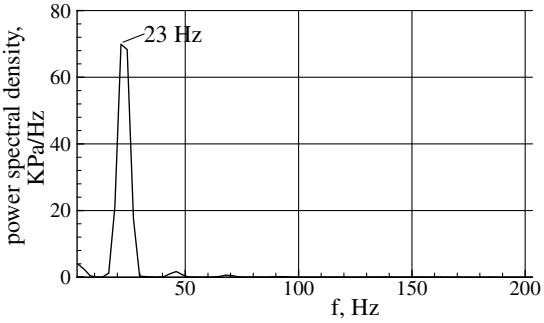

Fig. 12 Distribution of spectral density of instantaneous static pressure; the TR is 91%.

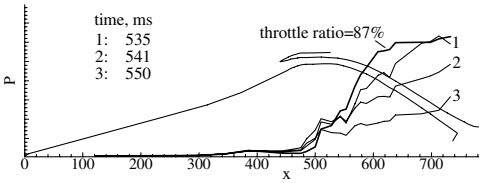

a) Shock system disgorging and swallowing

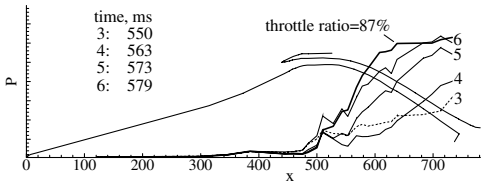

b) Near-throat flow pattern establishing and back pressure propagating

Fig. 13 Distributions of instantaneous static pressure along the central body-side at different typical moments; the TR is 91%.

and lasts for 15 ms unchangeably, which is coincident with the result obtained by shadowgraphs. The determinant factors of shock system disgorging and swallowing may include the arrangement of the outside compression shocks and the intensity of shock/boundary-layer interactions.

Time-history lines of static pressure at the throat of the inlet, the exit of the inlet, and the throat near the backplug are shown in Fig. 14, in which the throttling ratio is 91%. It can be seen clearly that the

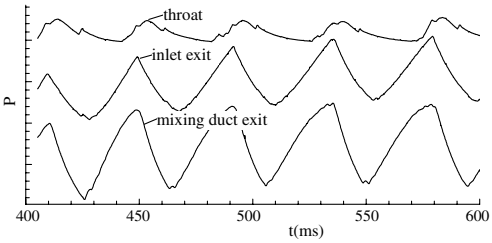

Fig. 14 Time-history lines of static pressure at typical stations; the TR is 91%.

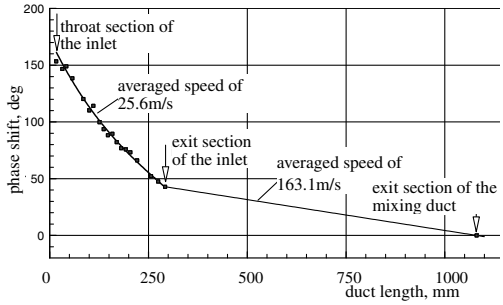

Fig. 15 Distribution of relative phase angles of static pressure along the internal flowpath; the TR is 91%.

pressure fluctuations increase as the monitoring station moves downstream. The pressure trough is formed near the backplug and propagates upstream at a certain speed. Figure 15 gives the relative phase angles of static pressures at each measurement station along the duct. As can be seen, the phase angle of each point has a positive value and increases as the station moves upstream, which verifies again that the pressure trough propagates upstream. Actually, the propagating speed can be calculated according to Fig. 15 as follows:

$$V_{\text{propagate}} = 360 \cdot f \cdot \mathrm{d}s/\mathrm{d}\phi$$

where f is the fundamental frequency, s is the propagating distance, and ϕ is the relative phase angle for which the unit is degrees. Results show that the pressure trough propagates upstream at a speed of 163.1 m/s in the straight mixing duct and at an average speed of 25.6 m/s in the diffuser of the inlet. The upstream propagating speed of weak disturbance equals $|u - c|$ and the variation of the cross-sectional area influences the average velocity u and then the speed of sound c of the duct flow, and so the difference of the propagating speeds is mainly caused by the variation of the cross-sectional area. Figure 15 indicates that the propagating speed increases with the cross-sectional area.

Conclusions

The aerodynamic instability of an unstable–unstarted hypersonic inlet, which is caused by the downstream mass flow choking at a Mach number of 6, is investigated with the aid of high-speed shadowgraphs and instantaneous pressure measurements. Two different throttling situations are investigated and both demonstrate strong unsteady flow characteristics. The results can be summarized as follows:

1) The shock system at the entrance of the inlet oscillates intermittently when the inlet is unstarted. With the increase of the throttling ratio, the fundamental frequency of the unsteady flow goes up and the shock-on-lip time go down, but the process whereby the shock system is disgorged and swallowed remains unchanged and lasts for 15 ms. When the throttling ratio is 89 and 91%, the fundamental frequency is 8 and 23 Hz, individually.

2) At the smaller throttling ratio, the unsteady flow cycle of the inlet can be divided into three stages: namely, mass filling up, shock system disgorging and swallowing, and near-throat flow pattern establishing and backpressure propagating. At the larger throttling ratio, the first process disappears and the third one is shortened.

3) When the shock system is disgorged, the mass that outflows from the duct is greater than that captured and a pressure trough is formed near the plug. The pressure trough propagates upstream at a speed of 163.1 m/s in the mixing duct and at a speed of 25.6 m/s in the diffuser of the inlet.

4) Static pressure of the internal flow fluctuates remarkably when the inlet is unstarted and the fluctuation scope is as high as 175 KPa at a condition of 3.0 MPa freestream total pressure.

5) When the inlet operates in an unstarted mode, intermittent reversed flow appears at the exit of the inlet and the proportion of the reversed flow period increases with the augment of the throttling ratio.

6) Normal shock, which is common in supersonic inlet buzz, was not observed in the oscillations of the shock system of an unstarted hypersonic inlet.

7) The inlet studied has the ability of self-starting at Mach 6.

Acknowledgment

This work is supported by National Nature Science Foundation of the People's Republic of China through grant no. 50606017.

References

[1] Curran, E. T., and Murthy, S. N. B., *Scramjet Propulsion*, Progress in Astronautics and Aeronautics, Vol. 189, AIAA, Reston, VA, 2001.

[2] Van Wie, D. M., Kwok, F. T., and Walsh, R. F., "Starting Characteristics of Supersonic Inlets," AIAA Paper 96-2914, July 1996.

[3] Andrews, E. H., McClinton, C. R., and Pinckney, S. Z., "Flowfield Starting Characteristics of an Axisymmetric Mixed-Compression Inlet," NASA TM-X-2072, Jan. 1971.

[4] ISGoldberg, T. J., and Hefner, J. N., "Starting Phenomena for Hypersonic Inlets with Thick Boundary Layers at Mach 6," NASA TN-D6280, Aug. 1971.

[5] Smart, M. K., "Experimental Testing of Hypersonic Inlet with Rectangular-to-Elliptical Shape Transition," *Journal of Propulsion and Power*, Vol. 17, No. 2, 2001, pp. 276–283.

[6] Kubota, S., Tani, K., and Masuya, G., "Aerodynamic Performance of a Combined Cycle Inlet," *Journal of Propulsion and Power*, Vol. 22, No. 4, 2006, pp. 900–904.

[7] Huebner, L. D., Rock, K. E., Ruf, E. G., Witte, D. W., and Andrews, E. H., Jr., "Hyper-X Flight Engine Ground Testing for Flight Risk Reduction," *Journal of Spacecraft and Rockets*, Vol. 38, No. 6, 2001, pp. 844–852.

[8] Zha, G. C., Knight, D., Smith, D., and Haas, M., "Numerical Simulation of High Speed Civil Transport Inlet Operability with Angle of Attack," *AIAA Journal*, Vol. 36, No. 7, 1998, pp. 1223–1229.

[9] Mayer, D. W., and Paynter, G. C., "Prediction of Supersonic Inlet Unstart Caused by Freestream disturbances," *AIAA Journal*, Vol. 33, No. 2, 1995, pp. 266–275.

[10] Scott, D. H., "Wind-Tunnel Blockage and Actuation Systems Test of a Two-Dimensional Scramjet Inlet Unstart Model at Mach 6," NASA TM-109152, 1994.

[11] Bao, W., Chang, J. T., Guo, X. G., and Cui, T., "Unstart Simulation of Scramjet Inlets," *Journal of Aerospace Power*, Vol. 20, No. 5, 2005, pp. 731–735.

[12] Yuan, H. C., and Liang, D. W., "Characteristic Analysis of Unstart Performance for Hypersonic Side-Wall Inlet Model," *Journal of Nanjing University of Aeronautics and Astronautics*, Vol. 36, No. 3, 2004, pp. 683–687.

[13] Rodi, P. E., Emamit, S., and Trexlers, C. A., "Unsteady Pressure Behavior in a Ramjet/Scramjet Inlet," *Journal of Propulsion and Power*, Vol. 12, No. 3, 1996, pp. 486–493.

[14] Newsome, R. W., "Numerical Simulation of Near-Critical and Unsteady, Subcritical Inlet Flow," *AIAA Journal*, Vol. 22, No. 10, 1984, pp. 1375–1379.

[15] Lu, P. J., and Jain, L. T., "Numerical Investigation of Inlet Buzz Flow," *Journal of Propulsion and Power*, Vol. 14, No. 1, 1998, pp. 90–100.

[16] Trapier, S., Duveau, P., and Deck, S., "Experimental Study of Supersonic Inlet Buzz," *AIAA Journal*, Vol. 44, No. 10, 2006, pp. 2354–2365.

[17] Oh, J. Y., Ma, F., Hsieh, S. Y., and Yang, V., "Interactions Between Shock and Acoustic Waves in a Supersonic Inlet Diffuser," *Journal of Propulsion and Power*, Vol. 21, No. 3, 2005, pp. 486–495.

R. Bowersox
Associate Editor